Heterogeneous Reaction of NO_3 with Ice and Sulfuric Acid Solutions: Upper Limits for the Uptake Coefficients

Frederick F. Fenter and Michel J. Rossi*

Laboratoire de Pollution Atmosphérique et Sol (LPAS), Swiss Federal Institute of Technology (EPFL), CH-1015 Lausanne, Switzerland

Received: January 9, 1997; In Final Form: March 25, 1997[⊗]

Using a Knudsen cell reactor, we have studied the uptake kinetics of the nitrate radical, NO_3, on ice and on sulfuric acid solutions. The experiments on ice were carried out over the temperature range $170 < T/K < 200$. Experiments with liquid sulfuric acid were performed over the concentration range 60−95 wt % H_2SO_4. Nitrate radical is detected by laser-induced fluorescence. Measures had to be taken to characterize the fluorescence quenching by water vapor, for which we found a bimolecular rate constant of $(6.9 \pm 0.5) \times 10^{-10}$ cm^3 molecule^{-1} s^{-1}. Also, the rate of NO_3 disappearance on the walls of the Teflon-coated reactor is determined and accounted for in the kinetic analysis. We find that, within the detection limit of our apparatus, there is no interaction between NO_3 and these surfaces, allowing us to report the upper limit for the uptake coefficient of $\gamma < 10^{-3}$.

Introduction

The nitrate radical, NO_3, is an important oxidizing species of the nighttime troposphere.[1] It has been detected in both the stratosphere[2] and the troposphere.[3,4] Notably, Platt et al., using differential optical absorption spectroscopy, have shown that under certain atmospheric conditions, the concentration in the troposphere can reach 10^9 cm^{-3}. The nitrate radical is known to react readily with unsaturated hydrocarbons such as olefins.[5] Over the past 10 years, serious efforts have been undertaken to study the homogeneous gas-phase reactivity of the nitrate radical in an attempt to better understand the role it plays as a nighttime oxidant. However, many aspects of nitrate radical atmospheric chemistry remain unexplored, including its reactivity with respect to commonly occurring atmospheric particulate. This aspect of nitrate radical chemistry is particularly important because of the evidence from field studies that reactions of NO_3 or N_2O_5 with atmospheric particulates might represent a significant loss of NO_x in the troposphere when the relative humidity exceeds 50%.[1,3,4] In a recent study by Rudich et al., the reactive uptake coefficient[8] of NO_3 on water and on ionic solutions was measured. They found γ values of 1.5×10^{-4} for pure water and up to 6×10^{-3} for the uptake on dilute solutions of chloride, bromide, and nitrite.[6] A better understanding of the heterogeneous reactivity of NO_3 is needed to assess the global importance of NO_3 as a nighttime oxidizing species. Here, we report experiments, conducted using a Knudsen cell reactor, on the heterogeneous reactivity of the NO_3 radical with two surfaces of atmospheric relevance. We have carried out kinetic measurements of the NO_3 interaction with ice over the temperature range $170 < T/K < 200$, as well as with liquid sulfuric acid solutions over the concentration range 60−95 wt % H_2SO_4.

Experimental Details

The Knudsen cell used in this study has been described in great detail in the recent literature.[7,8] It is a low-pressure flow reactor operated under molecular flow conditions. An isolation plunger allows the separation of the reactive surface of interest from the reactor volume so that control experiments can be performed. By analysis of the change in signal levels that occurs when a steady-state density of NO_3 is exposed to the ice or H_2SO_4 solution, a value for the net uptake probability can be calculated. Some specifications and relevant equations are summarized in Table 1. For all the experiments described here, the samples are mounted in a low-temperature support[8] that, by resistive heating and by passage of liquid nitrogen cooled air, permits the precise control of the substrate temperature within the low-pressure environment of the Knudsen cell. The support has the shape of a cylindrical cup, with 15 cm^2 of surface area at the base and with an equal surface area along the walls. The cup is coated with halocarbon wax (Series 15-00, Halocarbon Products). All other internal surfaces (i.e., the reference chamber) are coated with Teflon (Dupont, FEP 120-N suspension).

The source of NO_3 employed in this study is based on the thermal decomposition of N_2O_5. The N_2O_5 is prepared by oxidizing NO_2 with ozone with subsequent trapping and distillation at CO_2(s) (195 K) and N_2(l) (77 K) temperatures.[7] To generate the NO_3, the N_2O_5 is passed through a capillary heated externally using nichrome wire to about 530 K. Typical N_2O_5 flow rates are on the order of 10^{14} molecule s^{-1}, determined by measuring the pressure drop as N_2O_5 flows out of a calibrated volume as a function of time. In ancillary experiments, it was found that NO_2 does not interact with ice or sulfuric acid solutions under the selected experimental conditions. Laser-induced fluorescence measurements of the NO_2 generated inside the NO_3 source indicate that the thermal decomposition of N_2O_5 is nearly complete. Once inside the low-pressure flow reactor, any surviving N_2O_5 is thermally stable over the gas-phase residence time.

The NO_3 radical density is determined by laser-induced fluorescence at its absorption feature peaking near 662 nm. An optical sidearm allows for direct *in situ* detection inside the Knudsen cell. The laser light is generated by a pulsed Nd:YAG laser, doubled to the green (533 nm) and passed into a dye laser operated with DCM. The resulting output is about 30 mJ/pulse at 662 nm for a pulse repetition frequency of 10 Hz. The collimated laser beam, approximately 5 mm wide, is directed into the Knudsen cell via a quartz Brewster's angle

* To whom correspondence should be addressed.
⊗ Abstract published in *Advance ACS Abstracts,* May 1, 1997.

S1089-5639(97)00162-X CCC: $14.00

TABLE 1: Specifications and Relevant Kinetic Expressions

definition	symbol	value or expression
reactor volume	V	1840 cm^3
reactor surface area	A_R	2000 cm^2
sample surface area	A_S	15.2 cm^2
gas number density	N	$(1-1000) \times 10^{10}$ cm^{-3}
orifice diameters	D_O	1, 4, 8 mm
collision frequency (per cm^2)	Z_1	2.0 $(T/M)^{0.5}$ s^{-1} cm^{-2}
first-order rate constant (data analysis)	k_I	$(S_i/S_f - 1)k_{ref}$
rate constant of reference loss[a]	k_{ref}	$k_{esc} + k_{add}$
rate constants of effusive loss[b]	k_{esc} (1 mm)	$1.6 \times 10^{-2}(T/M)^{0.5}$ s^{-1}
	k_{esc} (4 mm)	$2.0 \times 10^{-1}(T/M)^{0.5}$ s^{-1}
	k_{esc} (8 mm)	$8.0 \times 10^{-1}(T/M)^{0.5}$ s^{-1}
rate constant of additional first-order loss	k_{add}	
signal levels for orifices A and B	S^A, S^B	measured in laboratory
initial and final signal levels	S_i, S_f	

[a] Sum of all first-order rate constants for NO_3 loss in the absence of the reactive surface. [b] Experimentally determined values for orifice diameters of nominal width.

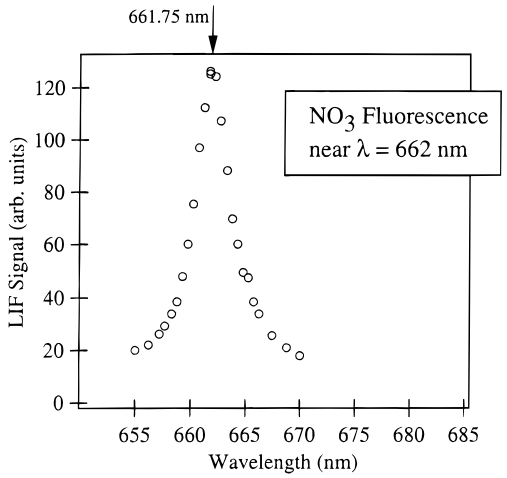

Figure 1. Laser-induced fluorescence excitation spectrum of NO_3 observed between 655 and 670 nm. The laser was passed unfocused through the Knudsen cell with a pulse energy of 30 mJ/pulse.

window. Using the known value for the cross section at 662 nm,[1] we calculate that this beam geometry leads to complete saturation of the NO_3 absorption. The resulting fluorescence is collected at right angles with respect to the propagating beam by using a planoconvex lens to collimate the fluorescence and a second planoconvex lens to focus the light through a small aperture (spatial filter) before impinging on a photomultiplier tube (Hamamatsu 928A). A 700 nm cutoff filter is used to protect the PMT from scattered laser light. The PMT signal is processed by a boxcar integrator with typical signal integration parameters of 2 μs delay, 200 ns gate width, and 10 shot averaging. At the 10 Hz laser repetition rate, this resulted in a reasonably fast signal response time (<3 s).

The LIF excitation spectrum of NO_3, as determined by varying the laser wavelength by increments of 0.5 nm, is shown in Figure 1. Because the N_2O_5 thermal source produces at least as much NO_2 as NO_3 radical, we have to subtract the contribution of NO_2 to the total LIF signal. This is done in a control experiment by adding a known flow of NO_2 to the cell and calibrating the response of the detection to the NO_2 fluorescence signal over the interval shown in Figure 1. The contribution of the NO_2 fluorescence to the total LIF signal observed at $\lambda = 661.75$ nm, where NO_3 is detected, is routinely subtracted and found to be always less than 5%.

Because sulfuric acid solutions and ice samples are both sources of gaseous water, we studied the quenching of NO_3 fluorescence by H_2O(g). In the absence of an external water flow, the lifetime of the NO_3 fluorescence was found to be on

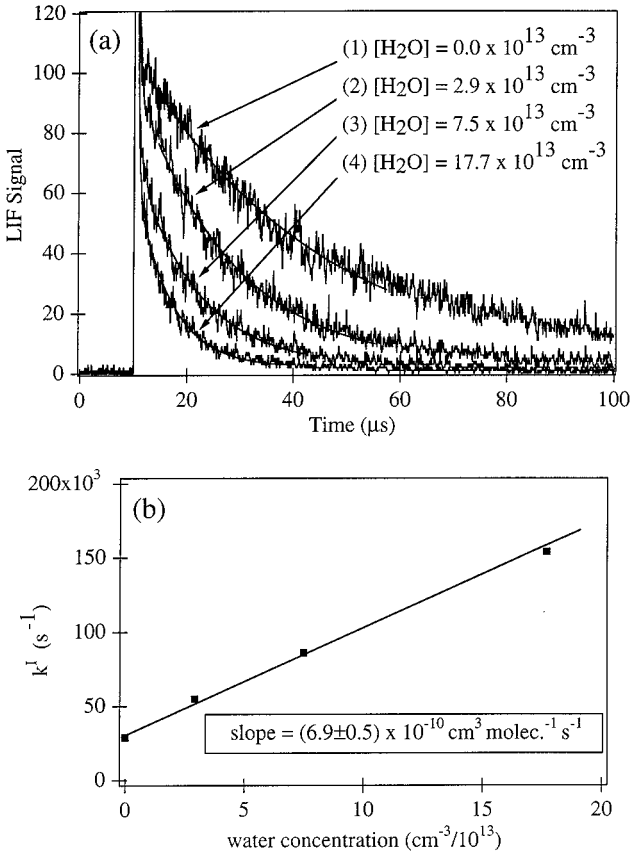

Figure 2. Quenching of NO_3 fluorescence by H_2O vapor. In (a), the real-time fluorescence profile is shown as a function of the gas-phase water density. When the pseudo-first-order decay rate constants are plotted as a function of the water vapor density, we obtain the quenching rate constant from the slope (b).

the order of 40 μs, which corresponds to the residence time of the NO_3 molecule within the optical detection volume. For our excitation conditions, the fluorescence lifetime of NO_3 is much longer than the 2 μs value reported by Ishiwata et al.[9] and is consistent with the value observed by McDonald et al., who reported a long-lived exponential tail corresponding to a lifetime of several hundreds of microseconds.[10] When measured flows of H_2O are introduced into the cell via a separate capillary, the NO_3 fluorescence is efficiently quenched, and the results of these experiments are shown and summarized in Figure 2. In Figure 2b, the pseudo-first-order decay rate constants are plotted as a function of the H_2O concentration and reveal an extremely fast bimolecular rate constant for the fluorescence quenching of NO_3 by H_2O(g) of $(6.9 \pm 0.5) \times 10^{-10}$ cm^3 $molecule^{-1}$ s^{-1} at ambient

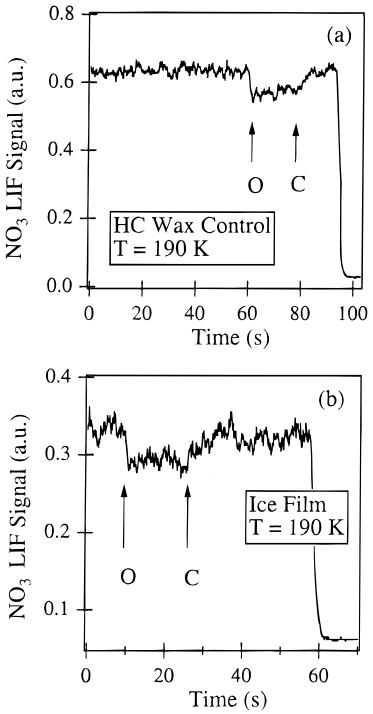

Figure 3. Typical experimental traces showing the interaction of NO_3 with respect to a halocarbon-wax-coated low-temperature support and an ice film of several micrometers thickness deposited on the same support. The value for the rate constant is determined from the change in signal levels using the appropriate expression given in Table 1. "O" and "C" refer to the lifting and lowering of the plunger that opens and closes the sample chamber of the Knudsen cell. The precipitous drop of the NO_3 LIF signal in (a) and (b) at $t = 90$ and 60 s, respectively, corresponds to the closing of the NO_3 source. At this time, the signal level does not fall to exactly zero because of the electronic offset of the boxcar aquisition.

TABLE 2: Summary of All Experiments

expt	substrate[a]	temp (K)	orifice (mm)	k_I [b] (s^{-1})	k_R [b] (s^{-1})
19jn	SA 95%	270	4	0.21	0.13
19jn	SA 95%	270	4	0.07	0.00
27jn	SA 60%	220	8	0.00	0.00
28jn	ice (B)	190	4	0.095	0.030
02jl	wax	190	4	0.15	
02jl	ice (D)	190	4	0.13	0.06
03jl	ice (D)	190	4	0.21	0.13
03jl	ice (D)	190	4	0.12	0.04
04jl	wax	190	4	0.16	
04jl	ice (D)	190	4	0.13	0.05
04jl	ice (D)	190	1	0.11	0.03
11jl	wax	190	1	0.10	
11jl	ice (D)	190	1	0.09	0.04
15jl	wax	190	4	0.45	
15jl	ice (D)	190	4	0.32	0.10
15jl	ice (D)	190	1	0.21	0.00
22jl	SA 60%	225	4	0.061	0.00
23jl	SA 80%	260	4	0.087	0.01
24jl	wax	300	4	0.21	
24jl	SA 95%	270	4	0.17	0.07
25jl	wax	180	4	0.16	
25jl	ice (D)	180	4	0.12	0.04
26jl	wax	170	4	0.16	
26jl	ice (D)	170	4	0.12	0.04
26jl	ice (D)	170	1	0.11	0.03
26jl	ice (D)	180	4	0.13	0.05
26jl	ice (D)	180	1	0.09	0.01
26jl	ice (D)	200	4	0.07	0.00
30jl	wax	300	4	0.22	
30jl	SA 60%	225	4	0.14	0.03
05au	SA 70%	230	4	0.13	0.02
06au	SA 95%	268	4	0.10	0.00

[a] For ice experiments, "D" refers to thin-layer deposited samples and "B" to bulk-added samples. [b] k_I and k_R are the observed and corrected values for the rate constant, respectively, as defined in the text.

temperatures. The experimental protocol for the measurement of the NO_3 uptake rate was selected to take into account the efficient quenching of NO_3 fluorescence by $H_2O(g)$.

A second experimental complication arises because NO_3 is found to disappear at a non-negligible rate on the Teflon-coated walls of the Knudsen cell reactor. For the kinetic analysis, the rate at which NO_3 disappears within the reaction volume is no longer determined exclusively by the rate of effusion via the escape orifice, which is one of the basic assumptions of the Knudsen cell technique. Fortunately, the additional loss process of NO_3 was found to be of first order with respect to the NO_3 density and constant over the course of days or weeks. The rate constant, referred to here as k_{add}, can be determined simply from the ratios of the steady-state signals measured at various exit-orifice diameters using the expression given in Table 1. For all the reported experiments, the first-order rate constant for NO_3 disappearance, k_{add}, is found to be in the range $(3.0 \pm 0.5) \times 10^{-1}$ s^{-1}.

With the potential systematic effects of fluorescence quenching and disappearance of NO_3 on the walls in mind, we developed a protocol for the measurement of the uptake coefficients of NO_3 on ice and on H_2SO_4(l). For uptake experiments on ice, the protocol is summarized in the following steps. (1) The empty wax-coated support is mounted and cooled to the desired temperature, isolated from the volume of the Knudsen cell. (2) The NO_3 flow is established and its interaction with the wax coating is measured in a control experiment, as shown in Figure 3a. (3) The NO_3 flow is stopped, and a H_2O flow is introduced using a separate inlet line to deposit an ice film on the wax coating. (4) After an ice layer of several micrometers thickness is deposited (determined from the measured deposition rate, deposition time, and the assumption that the density of the film is 1.0 g cm^{-3}), the flow is reduced to match the vapor pressure of the ice at the given temperature, i.e., the water flow is adjusted so that lifting and lowering the isolation plunger, thus opening and closing the sample compartment, do not alter the H_2O density inside the reactor. (5) The ice sample is isolated and the NO_3 flow reestablished, and the interaction between NO_3 and the ice is observed by following the NO_3 density change upon opening of the sample chamber, as shown in Figure 3b. The procedure for the H_2SO_4(l) experiments is similar. (1) The H_2SO_4 solution is prepared by dilution of a 95 wt % H_2SO_4 stock solution. (2) The H_2SO_4 is placed into the wax-coated support and cooled to the desired temperature, with the sample isolated from the reactor volume. (3) The H_2O flow required to achieve the equilibrium vapor pressure of the solution is introduced as above. (4) The sample is isolated, the NO_3 flow established, and the interaction of the NO_3 with the H_2SO_4(l) is monitored as the isolation plunger is lifted to expose the NO_3 to the cold H_2SO_4 surface.

All experimental results are given in Table 2. The temperature for each experiment had to be low enough to ensure that the total pressure in the cell remained in the molecular flow regime. Thus, for the NO_3 uptake experiments on ice the upper limit for the substrate temperature was 200 K, whereas liquid sulfuric acid concentrations could be studied up to ambient temperatures depending on the composition (see Table 2). The unpassivated halocarbon wax coating is found to be essentially inert with respect to NO_3, with an associated first-order rate constant for NO_3 disappearance of about 0.3 s^{-1}. The thin ice films and the H_2SO_4 solutions only cover the bottom part of

the sample support, and this area represents 50% of the total wax-coated surface exposed to NO_3 during the control experiment. To find the rate constant for NO_3 loss on the ice or acid solution (k_R), we must correct the observed rate constant (k_I) for the wax reactivity (k_{wax}), and this is done in the last column of Table 2:

$$k_R = k_I - 0.50k_{wax} \quad (1)$$

The value for k_{wax} is taken from the control experiment conducted at the beginning of each series of experiments and slightly changes from one experimental series to the next, and this is the reason for the chronological listing of Table 2. It should be noted that the reactivity of NO_3 is greater on the wax-coated surface ($k_{wax} \approx 0.3\ s^{-1}$ for a 30 cm^2 sample-dish surface) than on the passivated Teflon walls of the reactor ($k_{add} = 0.3\ s^{-1}$ for a 2000 cm^2 internal reactor surface area).

Results

From all the experiments summarized in Table 2, we conclude that the observed reactivity is due to the NO_3−halocarbon wax interaction and not to NO_3 interaction with the ice film or with the sulfuric acid solutions. Owing to the uncertainty involved in the characterization of the secondary heterogeneous processes, we prefer to report our conclusions in the form of upper limits. From all the experiments conducted on bulk water or on water ice films deposited from the vapor phase, we find that $k_R < (3.8 \pm 3.0) \times 10^{-2}\ s^{-1}$, corresponding to $\gamma < (6.1 \pm 4.7) \times 10^{-4}$, where the reported uncertainty is the 1σ limit of the average. We cast the rate constant k_R, which is the result of the present kinetic investigation, in the form of the dimensionless uptake coefficient γ according to the relation

$$\gamma = \frac{k_R}{Z_1 A_S} \quad (2)$$

We reach a similar conclusion for the experiments conducted on sulfuric acid solutions: averaging all the experiments that cover the entire concentration range studied, we obtain $k_R < (3.5 \pm 4.0) \times 10^{-2}\ s^{-1}$, corresponding to $\gamma < (6.0 \pm 6.8) \times 10^{-4}$. The results show that the uptake probability of NO_3 on ice or on sulfuric acid solutions, over the range of reported experimental conditions, is less than 10^{-3}.

Discussion and Conclusions

The experimental procedure, refined to take into account the complications of fluorescence quenching and NO_3 wall decomposition, has allowed us to determine upper limits for the heterogeneous reaction of NO_3 with the atmospherically important surfaces of ice and liquid sulfuric acid. Unfortunately, owing to the experimental complications associated with the secondary heterogeneous reactivity of NO_3, we can only state that these results are consistent with the measurements of Rudich et al. for the reactive uptake probability on pure water. Clearly, the atmospheric implications of our finding will only be revealed by an atmospheric modeling study. The weak heterogeneous reactivity of the NO_3 radical is not too surprising considering the field observations that relatively elevated concentrations of NO_3 can build up in the presence of significant aerosol loading if the relative humidity is less than 50%.[1,3,4] In this sense, the NO_3 radical behaves more like NO_2, which also demonstrates little or no interaction with sulfuric acid solutions and with ice surfaces, rather than like HNO_3, which is taken up with high probability on both of these substrates.

The very efficient quenching of the NO_3 fluorescence by water vapor is not suprising in light of the known rapid quenching of NO_2 fluorescence[11] by H_2O and of NO_3 fluorescence by HNO_3 and other gases.[9]

We are currently studying the reactivity of NO_3 with respect to other commonly occurring atmospheric particulates, such as amorphous carbon and salt, as part of our attempt to better understand the role of heterogeneous chemistry in the processing of nitrogen oxides in the earth's atmosphere.

Acknowledgment. This work was funded by the Fonds National Suisse de la Recherche Scientifique (FNS) under Grant Number 2000-43′353.95 and by the Office Fédéral de l'Education et de la Science (OFES) under the HALOTROP contract in the E.U. framework of the Environment and Climate Program. We are grateful to Professor Hubert van den Bergh for his support and lively interest.

References and Notes

(1) Wayne, R. P.; Barnes, I.; Biggs, P.; Burrows, J. P.; Canosa-Mas, C. E.; Hjorth, J.; Le Bras, G.; Moortgat, G. K.; Perner, D.; Poulet, G.; Restelli, G.; Sidebottom, H. *Atmos. Environ.* **1991**, *25A*, 206.

(2) Norton, R. B.; Noxon, J. F. *J. Geophys. Res.* **1986**, *91*, 5323.

(3) Platt, U.; Perner, D.; Winer, A. M.; Harris, G. W.; Pitts, J. N., Jr. *Geophys. Res. Lett.* **1980**, *7*, 89.

(4) Platt, U.; Winer, A. M.; Biermann, H. W.; Atkinson, R.; Pitts, J. N., Jr. *Environm. Sci. Technol.* **1984**, *18*, 365.

(5) Aschmann, S. A.; Atkinson, R. *Atmos. Environ.* **1995**, *29*, 2311.

(6) Rudich, Y.; Talukdar, R. K.; Ravishankara, A. R.; Fox, R. W. *J. Geophys. Res.* **1996**, *101*, 21023.

(7) Fenter, F. F.; Caloz, F.; Rossi, M. J. *J. Phys. Chem.* **1996**, *100*, 1008.

(8) Caloz, F.; Fenter, F. F.; Tabor, K. D.; Rossi, M. J. *Rev. Sci. Instrum.*, in press.

(9) Nelson, H. H.; Pasternack, L.; McDonald, J. R. *J. Chem. Phys.* **1983**, *79*, 4279.

(10) Ishiwata, T.; Fujiwara, I.; Narugi, Y.; Tanaka, I. *J. Phys. Chem.* **1983**, *87*, 1349.

(11) Okabe, H. *Photochemistry of Small Molecules*; Wiley-Interscience: New York, 1978.